# Nanomaching of Silicon nanoporous Structures by Colloidal Gold Nanoparticle

J. Zhu[*], H. Bart-Smith[**], M. R. Begley[**], R. G. Kelly[***], G. Zangari[***], and M. L. Reed[*]

[*]Department of Electrical and Computer Engineering,
[**] Department of Mechanical and Aerospace Engineering,
[***] Department of Materials Science and Engineering,
University of Virginia, Charlottesville VA 22904

## ABSTRACT

We report an efficient method for fabricating nanoporous structures in crystalline silicon, using colloidal gold nanoparticles in $HF/H_2O_2$ etchant. Colloidal gold in $HF/H_2O_2$ solutions accelerates the etching rate by two orders of magnitude and simultaneously introduces anisotropy in the etching process, with preferential penetration along the <100> directions. Random nanoporous structure, tailored nanochannel and nanopore were developed with this method.

***Keywords***: gold nanoparticle, nanoporous silicon

## 1 INTRODUCTION

Porous silicon has drawn a great deal of attention in applications such as optoelectronics [1], photonic crystals [2], optical filters [3], membranes and molecular sieves [4, 5]. Porous silicon is usually synthesized by electrochemical anodization in HF-containing aqueous or organic solutions [6-8]; its morphology is determined by the anodization conditions, the electrolyte chemistry, as well as the Si doping type and the dopant concentration. Certain morphologies, such as straight pores with narrow pore size distributions, can be obtained only under strictly controlled synthesis conditions [9]. Surface modification of silicon by the deposition of discontinuous metal films has been found to accelerate the etching process [10] and in some cases to generate straight pores [11]; however, the control of pore size by this method is limited and the lowest achievable dimensions are of the order of 50-100 nm. Here we demonstrate control of the nanostructure of porous silicon by nanoparticle-assisted etching of silicon in electrolytes containing HF and $H_2O_2$, which accelerates the etching rate by two orders of magnitude and simultaneously introduces anisotropy in the etching process, with preferential penetration along the <100> directions. The process does not require an external electrochemical cell or potentiostat and can thus be achieved without electrical leads and contacts.

## 2 POROUS SILICON FORMED WITH GOLD NANOPARTICLE ASSISTED ETCHING

Etching of silicon by immersion in HF/ $H_2O_2$ solutions occurs very slowly, at a rate of about 1 nm/min [12]. Inclusion of $H_2O_2$ in an HF solution decreases the surface roughness by rendering the etch process isotropic [13]. Addition of colloidal gold nanoparticles (AuNPs) to the HF/ $H_2O_2$ solution (AuNPs-HF/ $H_2O_2$), as we report here, results in a considerable enhancement of the silicon etching rate, up to approximately 100 nm/min. Additionally, the etching process in presence of the AuNPs is no longer isotropic. As shown later, this procedure can be used to synthesize porous silicon structures from starting material with different crystal orientations, as well as different doping types and concentrations.

The AuNPs used in this study were MesoGold from Purest Colloids, Inc. (Westampton, NJ), with a purity of 99.99% and a nominal diameter of 3.2 ± 0.3 nm. The etching solution (AuNPs-HF/$H_2O_2$) was a 10:5:1 mixture (by volume) of 10 ppm colloidal AuNPs in deionized water, 30% $H_2O_2$, and 49% HF (the latter two supplied by Mallinckrodt Baker, Inc., Mallinckrodt, NJ). The prepared etchant is stable at room temperature for several months.

Etching experiments were carried out on 2 inch diameter silicon wafers with various doping types, with a doping concentration ranging from $2\times10^{14}$ to $10^{20}$ $cm^{-3}$, and different orientations. After sequential spin cleaning with trichloroethylene, isopropanol, and methanol, the samples were lowered into a polypropylene beaker containing the AuNPs-HF/ $H_2O_2$, at room temperature, and a magnetic stirrer. After a timed etch, the samples were rinsed with deionized water and dried with nitrogen. Porous silicon regions formed on all silicon samples, as evidenced by scanning electron microscopy (SEM) images.

The electron micrographs in Fig.1 a-c (30, 60, 300 s etching, respectively) show the temporal evolution of the porous silicon region formed by this method on a P-type (001) Si substrate. During the early etching phases we observe pit formation at discrete locations. The etching paths increase in density and length until they cover the whole surface; a corresponding increase in surface roughness and depth of the porous silicon region results. In Fig. 1d, a tilted (10º) cross section reveals that the silicon has been converted to a porous region to a depth of approximately 150 to 200 nm. Control experiments, using



NSTI-Nanotech 2008, www.nsti.org, ISBN 978-1-4200-8503-7 Vol. 1

samples immersed in the HF/ $H_2O_2$ etchant without AuNPs, do not result in formation of any porous structures.

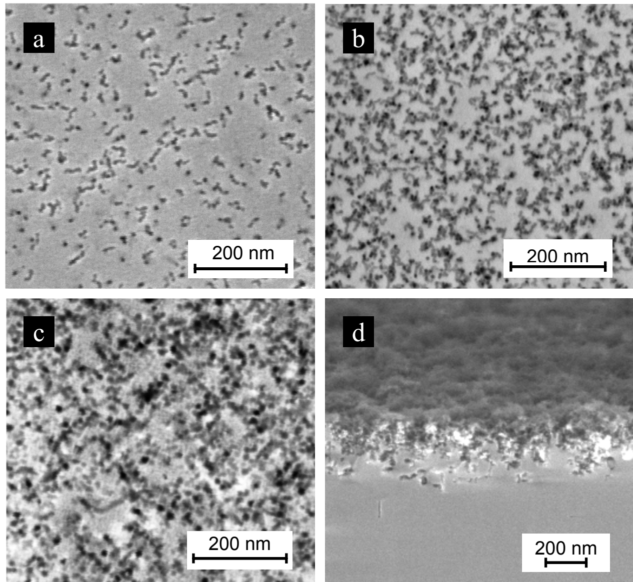


Figure 1: Scanning electron micrographs (SEM) of nanoporous network structures in p-type (001) silicon induced by colloidal gold nanoparticles (AuNPs) in an $HF/H_2O_2$ etchant. In a-c, the temporal evolution of the porous silicon formation is evident. a, 30 sec etching. b, 60 sec etching. c, 5 min etching. d. Cross sectional view [10° tilt] of the sample etched for 5 min, showing the porous silicon layer approximately 150 - 200 nm thick.

The SEM images in Fig. 1 suggest that the etching process results in the formation of channels with approximately uniform diameter into the Si. To clarify this observation, we fabricated arrays of porous silicon regions by patterning a Si surface using optical lithography. A hexagonal pattern of exposed Si regions approximately 1.2 μm in diameter was defined on a 600 nm thick thermally grown $SiO_2$ film. After a 300 s etch in the $HF/H_2O_2$ solution containing AuNPs, the oxide layer was stripped using a buffered HF solution. Examination of the surface, Fig. 2, shows the resulting porous silicon regions. As depicted in Fig. 2 a, for P-type (001) Si substrate, the edges of the etched circles are not sharp, but instead reveal a network of channels extending outwards, each about 20 nm wide, which are exclusively aligned along the [010] and [100] directions, both of which are in the plane of the (001) silicon surface.

We also observe that the nanometer sized channels in Fig. 2 a, which extend away from the edges of the porous silicon arrays, usually terminate with one of two different features. Bright end regions are indicated by black arrowheads, while dark end regions are indicated by white arrowheads. We hypothesize the former are AuNPs that have localized the dissolution along a <100>-oriented channel into the Si, while the later are vias through which the AuNPs escaped from or into the silicon surface by turning 90° into another <100> direction. Only one bright or one dark dot is observed along any single nanochannel, suggesting that the nanochannels are the result of penetration of AuNPs into the bulk Si.

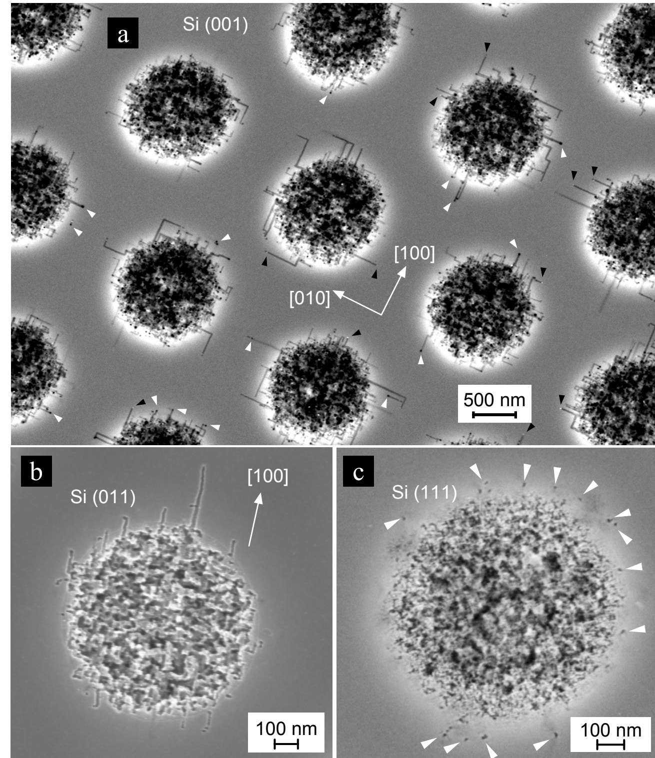


Figure 2: SEM of nanoporous Si arrays with different Si substrate orientations. Porous silicon patterns approximately 1.2 μm in diameter were fabricated by etching lithographically defined regions with $HF/H_2O_2$ solution containing AuNPs. a, For a (001) Si substrate, at the periphery of the etched areas are numerous nanochannels extending away from the porous regions, always along <100> directions. Two features are commonly observed at the ends of the nanochannels: bright areas, indicated by black arrowheads, and white areas indicated by white arrowheads. b, Nanochannels arising from penetration of AuNPs are in one direction only, the single <100> direction lying in the (011) surface plane of the silicon. c, No nanochannels extend from the periphery, consistent with the absence of <100> directions lying in the (111) surface plane. However we observe numerous nanometer-scale openings some distance away from the periphery; we interpret these as exit holes of nanochannels formed by localized dissolution along <100> directions by AuNPs that have penetrated into the Si bulk.

Confirmation of the preferred penetration along <100> was obtained by conducting experiments on Si wafers with other orientations. Fig. 2 b shows the result of etching an (011) oriented silicon substrate in the AuNPs-HF/ $H_2O_2$ solution for 5 min; nanochannels resulting from the AuNP penetration are oriented only in one direction, that of the single <100> direction that lies in the (011) surface plane.

Fig. 2 c shows the result of an etch experiment using a (111) oriented Si substrate; there are no nanochannels apparent on the wafer surface, consistent with the fact that no <100> directions lie in the (111) plane. However, we observe numerous small openings about 20 nm in diameter (indicated by arrowheads in Fig. 2 c) near the periphery of the masked region, but separated from the porous Si area. We interpret these as exit points for nanochannels formed by localized dissolution by the AuNPs in the bulk Si which have reemerged after making a 90° turn into another <100> direction.

## 3 DISCUSSION AND CONCLUSION

To further understand the influence of the AuNPs on the etching process, we prepared solutions of AuNPs in $HF/H_2O_2$ electrolytes using two other gold colloids, one synthesized in our laboratory following the method of Turkevich et al14, with average nanoparticle diameters of about 50 nm, and the other commercially available from Ted Pella Inc. (Redding CA), with nanoparticles having an average diameter of 25 nm. After 10 min immersion of silicon wafers into either of these solutions, no nanoporous structures formed.

We believe this lack of porous Si formation is due to the different adsorption behavior of the NPs onto the silicon surface. Gold nanoparticles in water or in weakly acidic solutions are usually negatively charged due to the presence of a citrate/acrylate stabilizing coat remaining after the manufacturing process [15]. This negative charge results in Coulombic repulsion from a silicon surface, which is negatively charged at these pH values [16]. When the pH is decreased, the citrate anions stabilizing the AuNPs are transformed into neutral citric acid, thus allowing adsorption to the silicon surface, while at the same time favoring agglomeration of the NPs. We tested the adsorption properties of the three types of AuNPs on silicon surface in 0.1% HF solutions. Our results show that, after 2 min of immersion, MesoGold NPs were adsorbed and uniformly dispersed on the silicon surface, Fig. 3a. In contrast, the other two types of AuNPs, with diameters of 50 and 25 nm, tended to aggregate when adsorbed on the silicon surface, Fig.3b.

We also investigated the influence of the HF concentration (from 0.1% to 2%) on the adsorption behavior of the MesoGold. We found that there is no significant change in the density of AuNPs adsorption in various HF: $H_2O$ solutions (no $H_2O_2$) for concentrations exceeding 0.1%, which indicates that a wide range of HF concentration will favor the AuNPs adsorption. The areal density of adsorbed AuNPs varied from 124 to 171 $m^{-2}$, much higher than those recently reported by Woodruff et al [16] (3 to 4 counts/$m^2$). The high density of adsorbed nanoparticles and the lack of aggregation may perhaps be explained in terms of the extremely small size of the MesoGold nanoparticles, which renders them more susceptible to Brownian scattering than to aggregation interactions.

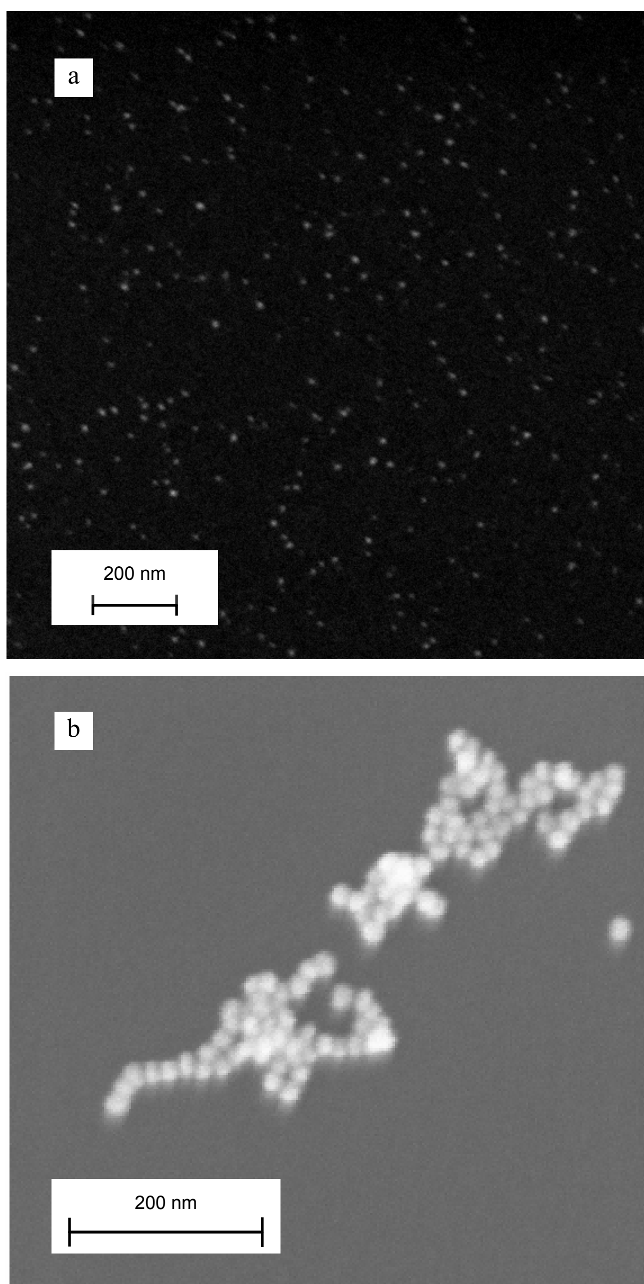


Figure 3: Colloidal gold nanoparticle adsorption on silicon in 1% HF solution. a, High density adsorption of 3.2 nm diameter AuNPs was achieved with the MesoGold colloids. b, 25 nm AuNPs from another source (Ted Pella Inc.) aggregated and covered the silicon surface at considerably lower density. Both SEM images were taken after 2 min of immersion, followed by rinsing with deionized water and drying with nitrogen.

We hypothesize that the etching process may be the result of the formation of local electrochemical cells at the silicon surface, induced by the presence of adsorbed AuNPs

and of hydrogen peroxide. In this scenario, the $H_2O_2$ is reduced to water at the adsorbed AuNPs, by the following reaction [17] in acidic solution:

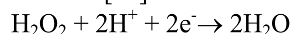

$H_2O_2 + 2H^+ + 2e^- \rightarrow 2H_2O$

The work function of AuNPs is about 5.4 eV within a wide range of particle diameter [18], which is higher than the electron affinity of silicon (4.05 eV). When AuNPs contact with crystalline silicon, it is energetically favorable for electrons to transfer from silicon to the nanoparticles, resulting in a more efficient reduction of hydrogen peroxide in the vicinity of the AuNPs. The migration of electrons at the AuNPs-Si contact also leaves behind compensating holes on silicon surface. The holes thus made available would promote silicon oxidation through the two possible reaction paths [19]:

$Si + 2h^+ \rightarrow Si^{2+}$ followed by $Si^{2+} + 2H^+ \rightarrow Si^{4+} + H_2$

or the direct oxidation:

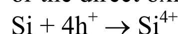

$Si + 4h^+ \rightarrow Si^{4+}$

In this way, the silicon atoms are etched and disappear into the etchant, as a soluble product such as $HSiF(OH)_2$ [20].

The overall process would be made possible by adsorbed AuNPs and would thus proceed in their proximity; the formation of elongated channels may consequently be explained by the fact that the AuNPs tend to remain localized at the regions that are being etched away. The preference for etching in the <001> direction can be explained in terms of the Current Burst Model by Föll’s group [21], whereby {111} pore surfaces are passivated at a higher rate, thus favoring etching along the <100> directions. Fluctuations in the kinetics of pore wall passivation would cause the observed occasional changes in the direction of the etching channel.

In summary, we have demonstrated an efficient method for producing porous silicon, capable of achieving very small and uniform pore sizes, without the need for an external electrochemical cell or potentiostat. This method may open up fruitful possibilities for developing controlled nanochannel networks in crystalline silicon.

## REFERENCES


[1] V. Lehmann, U. Gosele, Appl. Phys. Lett. 58, 856-858, 1991.

[2] S. R. Nicewarner-Pena, R. G. Freeman, B. D. Reiss, L. He, D. J. Pena, I. D. Walton, R. Cromer, C. D. Keating, M. J. Natan, Science 294, 137-141, 2001.

[3] V. Lehmann, S. Ronnebeck, Sens. Actuators, A, 95, 202-207, 2001.

[4] J. Fu, J. Yoo, J. Han, Phys. Rev. Lett. 97, 018103 , 2006.

[5] C. C. Striemer, T. R. Gaborski, J. L. McGrath, P. M. Fauchet, Nature 445, 749-753, 2007.

[6] D. R Turner, J. Electrochem. Soc. 105, 402-408 , 1958.

[7] A. Uhlir, Jr., Bell Syst. Tech. J. 35, 333-347, 1956.

[8] R. L. Smith, S. D. Collinsa, J. Appl. Phys. 71, R1-R22, 1992.

[9] H. Föll, M. Christophersen, J. Carstensen, G. Hasse, Mater. Sci. Eng. R 39, 93–141, 2002.

[10] X. Li, P. W. Bohna, Appl. Phys. Lett. 77, 2572-2574, 2000.

[11] K. Tsujino, M. Matsumura, Adv. Mater. 17, 1045-1047, 2005.

[12] S. Koynov, M. S. Brandt, M. Stutzmann, Appl. Phys. Lett. 88, 203107, 2006.

[13] N. Imou, T. Ishiyama, Y. Omuraa, J. Electrochem. Soc. 153, G59-66, 2006.

[14] J. Turkevich, P. C. Stevenson, J. A Hillier, Discuss. Faraday Soc. 11, 55-75, 1951.

[15] S. Diegoli, P. M. Mendes, E. R. Baguley, S. J. Leigh, P. Iqbal, Y. R. Garcia Diaz, S. Begum, K. Critchley, G. D. Hammond, S. D. Evans, D. Attwood, I. P. Jones, J. A. Preece, J. Exp. Nanosci. 3, 333-353, 2006.

[16] J. H. Woodruff, J. B. Ratchford, I. A. Goldthorpe, P. C. McIntyre, C. E. D. Chidsey, Nano Lett. 7, 1637-1642, 2007.

[17] A. K. Shukla, R.K. Raman, Annu. Rev. Mater. Res. 33, 155–68, 2003.

[18] M. Schnippering, M. Carrara, A. Foelske, R. Kötz, D. J. Fermín. Phys. Chem. Chem. Phys. 9, 725-730, 2007.

[19] X. G. Zhang, J. Electrochem. Soc. 151, C69-C80, 2004.

[20] P. Allongue, V. Kielinc, H. Gerischer, Electrochimca Acta. 40, 1353-1360, 1995.

[21] C. Jager, B. Finkenberger, W. Jager, M. Christophersen, J. Carstensen, H. Foll, Mat. Sci. Eng. B 69, 199-204, 2000.